Participation of chromophore pairs in photoinduced intramolecular electron transfer for a naphthalimide spermine conjugate

Guilford Jones, II*, Satish Kumar

Department of Chemistry and Photonics Center, Boston University, Boston, MA 02215, USA

Abstract

Photophysical and electron transfer properties of the conjugate of 1,8-naphthalimide and spermine (BNS) and related chromophore system including, N-propyl-1,8-naphthalimide (NAP), have been investigated. Absorption and emission spectra for the BNS-spermine derivative revealed a ground state intramolecular complexation of the two naphthalimide chromophores, particularly for aqueous media. Fluorescence quenching studies of BNS using an electron donor, 1,4-diazabicyclo[2,2,2]octane (DABCO), yielded quenching rate constants near that anticipated for a diffusion-controlled process. Transients observed on laser flash photolysis ($\lambda_{exc} = 355$ nm) corresponding to the naphthalimide radical anion ($\lambda_{max} = 410$ nm) and the triplet state of BNS ($\lambda_{max} = 470$ nm) have been identified. Observation of a lower fluorescence quantum yield (in comparison to NAP) and the appearance of the radical anion intermediate on laser flash photolysis in the absence of any external electron donor (e.g., for BNS in its free base form) suggests a mechanism of intramolecular electron transfer involving either (a) interaction of two naphthalimide chromophores or (b) interaction of naphthalimide groups and a dialkyl amine moiety.
© 2003 Elsevier B.V. All rights reserved.

Keywords: Naphthalimide photochemistry; Spermine conjugate; Laser flash photolysis; Electron transfer

1. Introduction

Electron transfer reactions have been a target of research for several decades due to their importance in natural processes such as photosynthesis and aerobic respiration and in photonics applications including biosensors [1–3]. Special efforts have been directed recently toward design of self-assembling macromolecular systems capable of intramolecular electron transfer (e.g., de novo photoactive peptides) [4–8]. Other natural products or mimics that are capable of molecular recognition, such as polyamine derivatives, have been the focus of numerous investigations due to their important biological or medicinal properties. These molecules, such as spermine, exist as polycations at physiological pH, which accounts for their strong affinity for negatively charged species such as DNA [9] and lipopolysaccharides [10]. Naphthalimide conjugates of polyamines have received attention because of their antitumor activity [11–13]. Furthermore, photochemical properties of naphthalimide and naphthaldiimides are of special interest since they can cause site-specific or non-specific cleavage in oligonucleotides. Saito et al. [14] demonstrated

photoinduced DNA cleavage via electron transfer between a guanine base and 1,8 naphthalimide. Using laser flash photolysis methods, Aveline et al. [15], have characterized the photochemistry of various N-substituted 1,8-naphthalimide and 1,4,5,8-naphthaldiimides. In another recent investigation [16], photoinduced electron transfer for a naphthalimide that is covalently linked to a viologen was investigated as well.

The photochemical properties of polyamine–naphthalimide conjugates have not been studied to date. In this paper, the behavior of the N,N'-bis-1,8-naphthalimide-spermine conjugate (BNS) is reported. Model compounds, N-propyl-1, 8-naphthalimide (NAP) and N-(N-methylpropyl)-1,8-naphthalimide (MNP), each of which lacks either appended amine groups or the bichromophore moiety, have been studied as well for comparison. Absorption and emission data indicate that BNS forms an intramolecular chromophore dimer in polar solvents. Transient absorption spectroscopy ($\lambda_{exc} = 355$ nm) has been employed to identify the naphthalimide triplet and the radical anion that are associated with the folded species. In particular, we have discovered that dimer structure facilitates formation of the naphthalimide radical anion phototransient. The photochemistry of these intramolecular dimers may be useful in terms of the construction of amphiphilic assembly systems (e.g.

* Corresponding author. Tel.: +1-617-353-8656; fax: +1-617-353-7271.
E-mail address: jones@chem.bu.edu (G. Jones II).

spermine-polypeptide docking motifs) [17] that depend on electrostatic and hydrophobic interactions.

2. Experimental

2.1. Materials

1,8-Naphthalic anhydride, *N*-methyl-1,3-propanediamine, propylamine, and diethylamine were purchased from Aldrich and used as received. Spermine (Acros) was used without further purification. 1,4-Diazabicyclo[2,2,2]octane (DABCO) (Aldrich) was recrystallized from ethanol prior to use. Spectroscopic grade acetonitrile was obtained form J.T. Baker. Ethanol (200-proof) was supplied by Pharmco. Milli-Q deionized water was used in preparation of aqueous samples. The BNS (free base) and NAP were following reported procedures [11]. The physical and spectroscopic data are collected as follows.

2.1.1. N,N′-bis-1,8-naphthalimide spermine conjugate (BNS)

White solid, m.p. 172–174 °C; ^{1}H NMR (CDCl$_3$, 400 MHz) δ 8.58 (d, 4H, $J = 7.2$ Hz), 8.20 (d, 4H, $J = 8.0$ Hz), 7.66 (t, 4H, $J = 8.0, 7.2$ Hz), 4.23 (t, 4H, $J = 7.0$ Hz), 2.67 (t, 4H, $J = 6.8$ Hz), 2.59 (s, 4H), 1.93 (m, 4H), 1.49 (s, 4H); ^{13}C NMR (CDCl$_3$, 270 MHz) δ 164.2 (4C), 133.8 (4C), 131.5 (2C), 131.2 (4C), 128.0 (2C), 126.9 (4C), 122.5 (4C), 49.7 (2C), 47.0 (2C), 38.2 (2C), 28.3 (2C), 27.8 (2C); LRMS (CI, 70 eV) m/z (relative intensity) 563.2 [$(M + 1)^+$, 44.78], 326.0 (24.43), 307.1 (90.25), 255.0 (45.89), 198.0 (100); HRMS (CI, 70 eV) m/z 563.2621 $(M + 1)^+$, Calcd. for C$_{34}$H$_{34}$N$_4$O$_4$M$^+$ 562.2579.

2.1.2. N-propyl-1,8-naphthalimide (NAP)

Light yellow solid, m.p. 162–164 °C; ^{1}H NMR (CDCl$_3$, 400 MHz) δ 8.58 (d, 2H, $J = 7.3$ Hz), 8.19 (d, 2H, $J = 8.2$), 7.73 (t, 2H, $J = 7.3, 8.2$ Hz), 4.14 (t, 2H, $J = 7.6$), 1.75 (m, 2H), 1.00 (t, 3H, 7.4 Hz); ^{13}C NMR (CDCl$_3$, 300 MHz) δ 164.2 (2C), 133.7 (2C), 131.6, 131.1 (2C), 128.1, 126.9 (2C), 122.8 (2C), 41.9, 21.4, 11.5; LRMS (CI, 70 eV) m/z (relative intensity) 241.1 [$(M+2)^+$, 7.09], 240.1 [$(M+1)^+$, 72.16], 239.1 (M$^+$, 98.53), 197 (100.0), 180 (82.17), 153 (67.65), 152.1 (71.63); HRMS (CI, 70 eV) m/z 239.0958 M^+ found, Calcd. for C$_{15}$H$_{13}$NO$_2$M$^+$ 239.0946.

2.1.3. N(N-methylpropyl)-1,8-naphthalimide (MNP)

A mixture of 1,8-naphthalic anhydride (0.8 g, 4.0 mmol) and *N*-methyl-1,3-propanediamine (0.356 g, 4.8 mmol) was dissolved in toluene (15 ml) and heated under reflux for 4 h. A yellow solid (1.01 g) was obtained on evaporating the solvent under reduced pressure. Further purification by flash chromatography (SiO$_2$, 5% MeOH, 3% triethylamine/CH$_2$Cl$_2$) gave 0.778 g (72%) of a yellow solid, which on re-crystallization from dichloromethane-hexanes gave a light yellow crystalline solid (m.p. 107–108 °C);

^{1}H NMR (CDCl$_3$, 400 MHz) δ 8.59 (d, 2H, $J = 7.3$ Hz), 8.20 (d, 2H, $J = 8.2$ Hz), 7.74 (t, 2H, $J = 8.3, 7.3$ Hz), 4.25 (t, 2H, $J = 7.1$ Hz), 2.66 (t, 2H, $J = 6.9$ Hz), 2.43 (s, 3H), 1.94 (m, 2H); ^{13}C NMR (CDCl$_3$, 270 MHz) δ 164.1 (2C), 133.8 (2C), 131.5, 131.2 (2C), 128.1, 126.8 (2C), 122.6 (2C), 49.3, 38.3, 36.4, 28.2; LRMS (EI, 70 eV) m/z (relative intensity) 268.3.2 [$(M + 1)^+$, 8.06], 18.1 (17.9), 180.1 (21.7), 152.1 (23.8), 70.1 (100) HRMS (EI, 70 eV) m/z 268.1191 M^+, Calcd. for C$_{16}$H$_{16}$N$_2$O$_2$M$^+$ 268.1211.

2.2. Instrumentation and general methods

Absorption spectra were recorded on a Beckman DU-640B spectrophotometer. Steady-state emission and time-resolved measurements were obtained using a PTI (Photon Technology International, Inc.) fluorometer which employed Felix/Timemaster software. Fluorescence quantum yield measurements were carried out using dilute solutions (OD < 0.12) and referenced against NAP in ethanol (0.037) [18]. Fluorescence lifetimes were recorded using the PTI nitrogen laser source ($\lambda_{exc} = 337$ nm).

A tunable laser system (Continuum) pumped by a Q-Switched Nd:YAG laser (Surelite II-10) was used as excitation source in laser flash photolysis experiments. The repetition rate was 10 Hz with a 15 mJ/pulse with $\lambda_{exc} = 355$ nm. Control of the apparatus and the recording of data were performed using LabView 5.0 (National Instruments) (see [19] for further details). Experiments were carried out using freshly prepared solutions of BNS (36 μM) and NAP (99 μM). Solutions were deaerated as required by purging with argon for 30 min. Transient spectra were initially obtained for the full spectral range. Then transient decay or bleach profiles were monitored at peak maxima or minima. Decay curves were analyzed using Igor Pro 3.12 software using mono- and bi-exponential functions to describe growth and decay curves. All measurements were repeated several time and lifetimes are ±20%.

Cyclic voltammograms were recorded using a model 273A potentiostat/galvanostat (EG&G APR) controlled by an EG&G M270A (version 4.0) software package (scan rate was 1000 mV/s). All electrochemical measurements were performed using anhydrous acetonitrile containing 2.0 mM dye and 0.1 M tetrabutylammonium hexafluorophosphate. The reference electrode (Ag/AgCl) was calibrated using 5.0 mM ferrocene in dry acetonitrile (0.307 V vs. SCE, 0.2 M LiClO$_4$) [20]. Solutions were purged with argon (20 min) before recording current–voltage curves.

3. Results and discussion

3.1. Absorption and emission properties

Absorption and emission spectra of NAP and BNS (Scheme 1) were recorded in selected solvents; various

BNS

NAP

MNP

DABCO
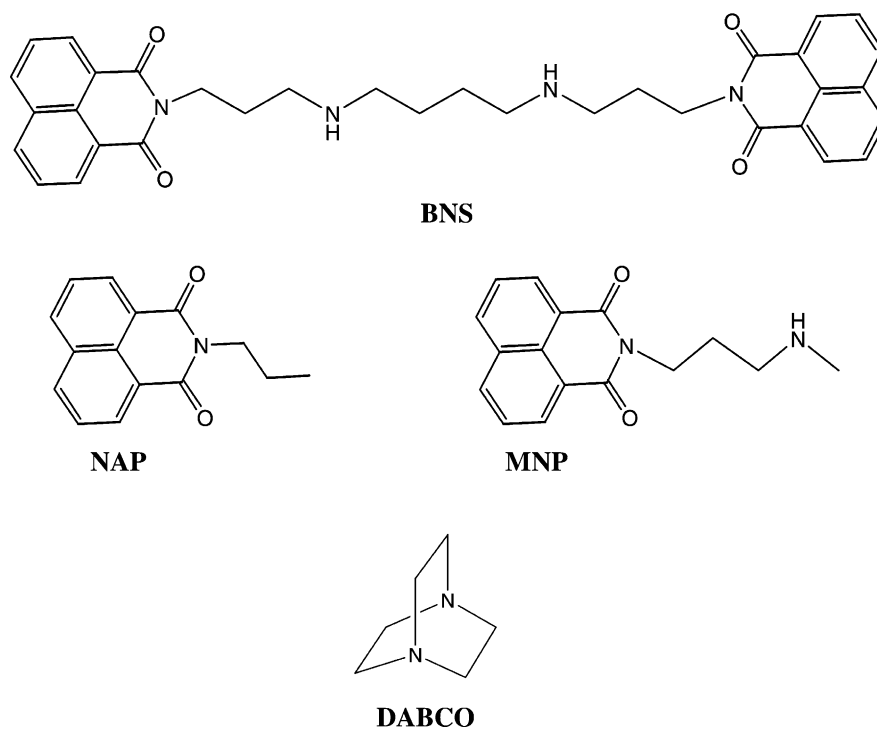
Scheme 1.

spectral parameters are listed in Table 1. Fig. 1 shows absorption spectra of NAP, MNP and BNS in water (pH = 7.4, 2.0 mM phosphate buffer). In Fig. 2 emission spectra of BNS and NAP have been shown in selected solvents. For BNS, measurements were carried out using the free base form unless otherwise indicated, or in the case in which water is the solvent, where the state of the protonation is dictated by the pH (for spermine values of $pK_a = 9.79$ and 8.90) [21]. A principal absorption band was observed in the

UV that depended moderately on solvent polarity (λ_{max} = 330–345 nm). The absorption spectrum of BNS (especially in water) is slightly broader compared with that of NAP and MNP. Furthermore, the peak extinction coefficients of BNS are lower than twice the values for NAP (a hypochromic effect). This result indicates that BNS participates to varying degrees in ground state interactions between naphthalimides, causing broadening of the UV absorption feature and a nominal lowering of the observed ε_{max} (although not the

Table 1
Photophysical spectral parameters of BNS and NAP in various media[a]

Solvent	λ_{abs} (nm)	$\varepsilon \times 10^{-4}$ (M^{-1} cm^{-1})	λ_{flu} (nm)	ϕ[b]	Lifetime (ns)[c]	
					Monomer	Dimer
BNS						
CH$_3$CN	331	2.18	377, 469	0.0093	<0.40	8.8
CH$_3$CN/TFA[d]	331	2.27	377, 469	0.045	<0.40	15.0
H$_2$O (pH = 10.6)[e]	342	1.71	395, 484	0.023	0.78	7.6
H$_2$O (pH = 7.4)[e]	343	1.70	395, 489	0.042	0.83	16.0
NAP						
CH$_3$CN	331	1.27	376	0.016	<0.40	
CH$_3$CN/TFA[d]	331	1.28	376	0.015	<0.40	
H$_2$O (pH = 10.6)[e]	345	1.28	395	0.21	2.2	
H$_2$O (pH = 7.4)[e]	344	1.23	395	0.21	2.3	

[a] Aerated room temperature solutions.
[b] Quantum yield for total emission recorded at 340–623 nm, $\lambda_{exc} = 317$ nm, quantum yield standard: NAP in ethanol (0.037) [17].
[c] Fluorescence lifetimes measured at 395 nm (water) or 377 nm (acetonitrile) for monomer and 495 nm (water) or 469 nm (acetonitrile) for dimer, $\lambda_{exc} = 337$ nm (nitrogen laser).
[d] [TFA] = 1.7 mM.
[e] 2.0 mM buffer solutions.
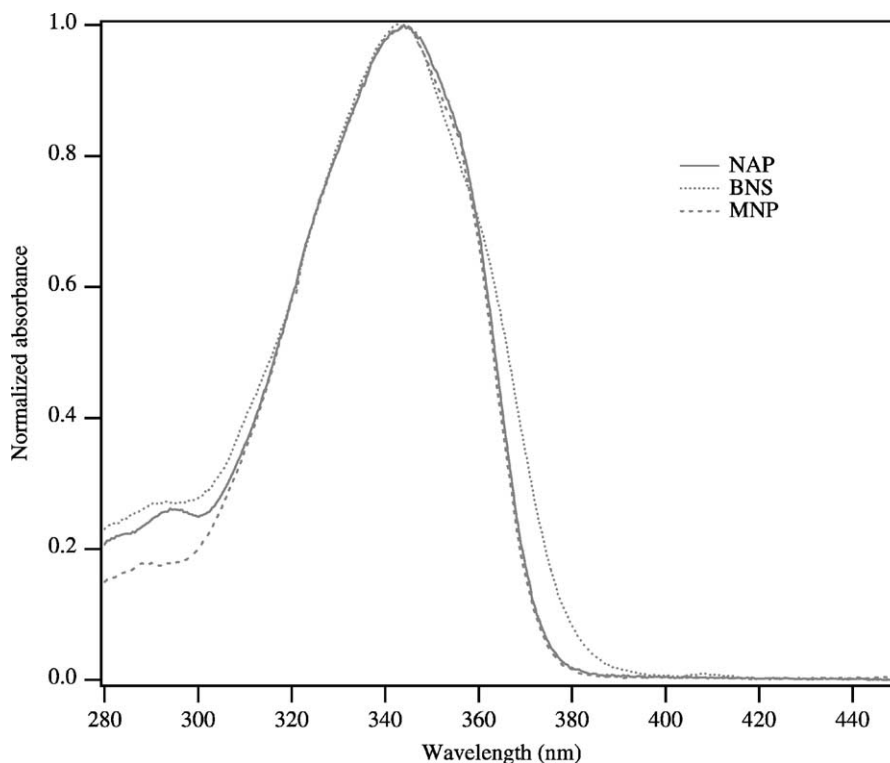
Fig. 1. Normalized absorption spectra for NAP, MNP and BNS (10–20 μM) in water (pH = 7.4, 2.0 mM phosphate buffer).

integrated intensity). In addition, the emission spectrum of BNS shows a structured band around 390 nm as observed for NAP along with an additional broad featureless band at longer wavelength (ca. 490 nm). Observation of a similar emission spectrum for concentrations of the conjugates as low as 250 nM rules out any intermolecular process of chromophore aggregation. This broad red-shifted emission, which is most prominent in water (Figs. 2 and 3), is ascribed to an intramolecular dimer formed between two naphthalimide chromophores. Dimer absorption apparently overlaps monomer absorption. The relative emission intensity of peaks at 395 and 489 nm depends on the excitation wavelength; the dimer ("excimer") is enhanced in intensity on excitation toward the red edge of BNS absorption (compare Figs. 2 and 3). For water–ethanol mixtures, dimer emission decreases as ethanol content increases due to a decrease in solution polarity which disfavors aggregation (i.e., chromophore pi stacking).

For acetonitrile solutions, the fluorescence quantum yield obtained for BNS is about twofold lower than the value obtained for NAP. On acidification of an acetonitrile solution of BNS (with 1.7 mM trifluroacetic acid), the fluorescence quantum yield is augmented about fivefold. For neutral water solutions (pH = 7.4) the fluorescence yield for BNS is increased about twofold over solutions held at pH = 10.6 (Fig. 3 and Table 1). Acidification of acetonitrile or water solutions did not alter the fluorescence quantum yield for the model compound, NAP.

In general, a lower emission quantum yield for BNS may be most readily ascribed to either of two processes: (1) photoinduced electron transfer from a dialkylamine moiety to the naphthalimide chromophore or (2) aggregation of two naphthalimide chromophores (before or following excitation) yielding an intramolecular dimer that has a low fluorescence quantum yield. The latter process is the apparent mechanism for water solutions at pH = 7.4, where both of the secondary amines in BNS are protonated. For NAP, an increase in fluorescence yield is observed upon changing the medium from acetonitrile to water, a finding consistent with reported work [22] on similar compounds.

Fluorescence lifetimes associated with monomeric emission for both BNS and NAP in acetonitrile were recorded at <0.4 ns (near the instrumental limit of resolution) (Table 1). In the case of water samples, monomer emission lifetimes were readily distinguished with a decrease, by a factor of 3, for BNS in comparison to NAP. The dimer emission observed for BNS in acetonitrile was not well resolved from monomer fluorescence and showed biphasic decay; the decay rate for the longer lived component of the weaker emitting dimer could be determined only approximately but was clearly increased for BNS in acidified acetonitrile (Table 1). The longer emission lifetimes recorded for BNS showed a single exponential decay in water, where dimer and monomer emission are well resolved; dimer lifetime increased about twofold on acidification.
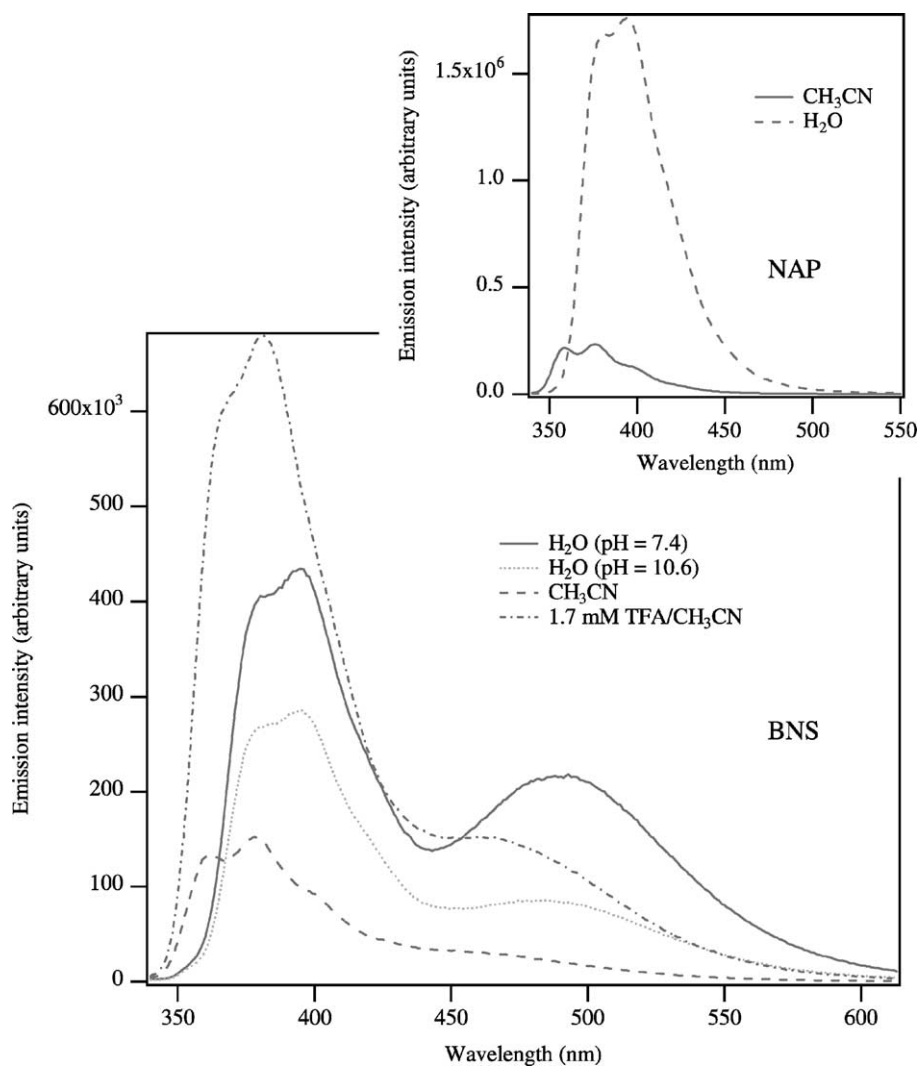
Fig. 2. Emission spectra obtained for emission of BNS (10–15 μM) in different media (blue edge excitation, $\lambda_{exc} = 317$ nm). Inset: emission spectra of NAP (20 μM) in acetonitrile and water.

3.2. Photoinduced electron transfer processes

3.2.1. Fluorescence quenching studies

The free energy change associated with electron transfer for the excited singlet state (S_1) of the spermine conjugate was evaluated using the Rehm–Weller equation (1) [23]:

$$\Delta G_{et} = F(E_{ox}^0 - E_{red}^0) - E_{00} - \frac{e^2}{\varepsilon r} \tag{1}$$

where E_{ox}^0 and E_{red}^0 are oxidation and reduction potentials for the donor and the acceptor, respectively, and E_{00} denotes the excitation energy. A contribution from the coulombic term was assigned for acetonitrile ($e^2/\varepsilon r = 0.1$ eV).

In the case where an excited chromophore NP undergoes electron transfer with a paired ground state NP, the following equation can be used to show the relation between E_{00} energy and the oxidation and reduction potentials of the chromophore [24]:

$$F(E_{ox}^0 - E_{red}^0) = E_{00} + k \tag{2}$$

where k is a contribution from exchange and coulomb repulsion interactions, configuration interaction energy and difference in solvation energies between radical ions and neutral species. On combining Eqs. (1) and (2) one obtains the following equation for ΔG_{et} associated with the formal process associated with intra-dimer electron transfer, NP* + NP → NP$^{\bullet +}$ + NP$^{\bullet -}$:

$$\Delta G_{et} = k - \left(\frac{e^2}{\varepsilon r}\right) \tag{3}$$

It can be concluded that in a self-oxidation–reduction process contributions from k and $e^2/\varepsilon r$ terms, even though generally small in value, will dictate the feasibility of the process. Photoinduced electron transfer in an acylpyrene chromophore aggregated via attachment to an amphiphilic polypeptide assembly has been recently reported [25]. In this case an electron transfer between an acylpyrene excited
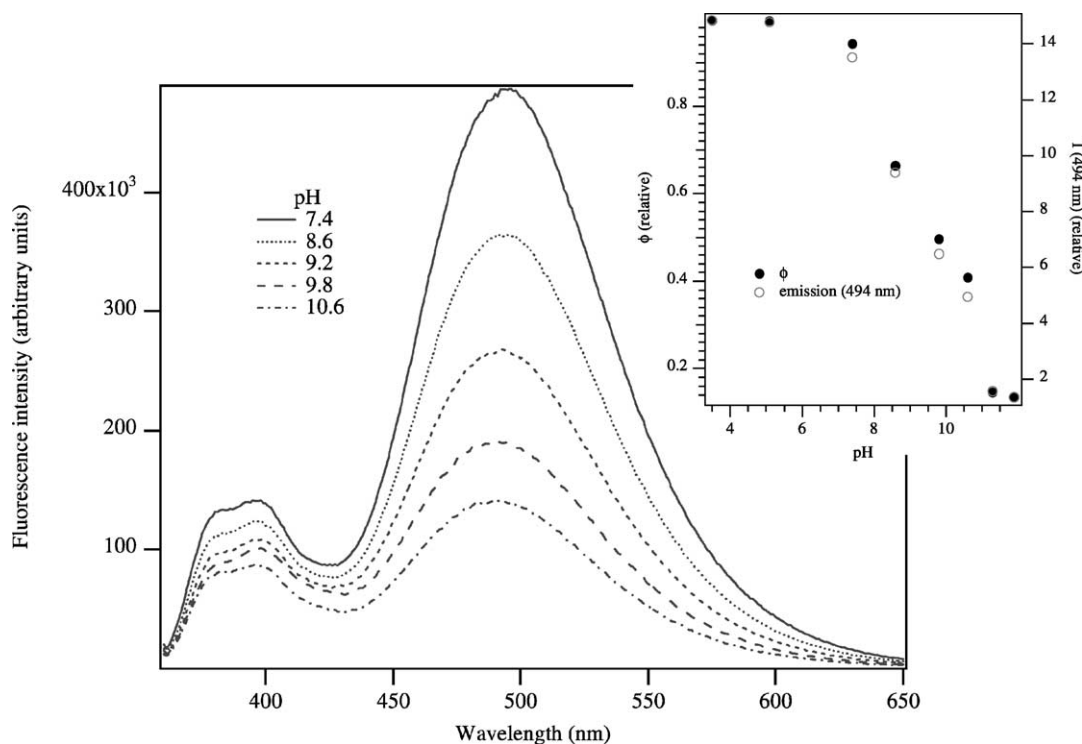
Fig. 3. Emission of BNS (10 µM) in water at varied pH (2 mM—phosphate or glycine/NaOH buffers or NaOH/HCl solutions) (λ_{exc} = 355 nm). Inset: titration curves obtained from monitoring relative fluorescence quantum yield, ϕ, (360–650 nm) or fluorescence intensity, I (494 nm).

singlet state and paired (aggregated) ground state acylpyrene chromophore was proposed.

The reduction potential of BNS measured using cyclic voltammetry was found to be -1.44 V vs. SCE (acetonitrile). The fluorescence emission, corresponding to BNS monomer and dimer, diminishes on increasing the pH of water solutions from 7.4 to 10.6 (Fig. 3) (emission spectra were corrected for the slight change in absorbance at excitation wavelength). This result is consistent with a mechanism in which secondary amines (the spermine chain) that assume the free base (unprotonated) form (E_{ox} = 1.31 V vs. SCE) [26] take part in an electron transfer process. The free energy changes for the reaction involving BNS monomer and dimer and secondary amine (using the value of -1.44 vs. SCE for monomer or dimer reduction) are calculated to be -0.86 and -0.59 eV, respectively. A diffusion-controlled fluorescence quenching for NAP in acetonitrile was observed on addition of diethylamine (k_q = 4.9×10^{10} M^{-1} s^{-1}). These findings for the model compound further support the hypothesis regarding electron transfer quenching of NP by an amine function that occurs in an intramolecular fashion for BNS. Assuming that the reduction in fluorescence yield and lifetime is the result of amine quenching, for BNS dimer in water (pH = 10.6), the electron transfer rate constant for intramolecular quenching (k_{et}) was computed to be 6.8×10^{7} s^{-1} using the following equation:

$$k_{et} = \frac{1}{\tau_{\text{deprotonated BNS}}} - \frac{1}{\tau_{\text{protonated BNS}}} \tag{4}$$

The increased non-radiative decay rate constant (i.e., via excimer formation) for BNS monomer in its protonated form in water (6.8×10^{8} s^{-1}, pH = 7.4) was calculated by comparing decay times for NAP and BNS monomer emission and using the relation:

$$k_{et} = \frac{1}{\tau_{\text{BNS}}} - \frac{1}{\tau_{\text{NAP}}} \tag{5}$$

Additional fluorescence quenching studies of NAP and BNS were conducted using another well known electron donor, DABCO (0.68 V vs. SCE) [27]. The driving force for electron transfer from DABCO to the naphthalimide excited singlet state is computed to be -1.49 eV for acetonitrile solvent. The free energy change involving the naphthalimide triplet state (E_T = 52.8 kcal/mol, 2.29 eV) [28] is small (-0.27 eV) but sufficient for this alternate process to occur (see flash photolysis results below). Stern–Volmer constants were obtained from fluorescence quenching data, 7.7 M^{-1} (k_q = 4.5×10^{10} M^{-1} s^{-1}) and 16 M^{-1} (k_q = 4.8×10^{10} M^{-1} s^{-1}) for the quenching by DABCO of NAP and BNS, respectively. This behavior is consistent with a diffusion-controlled electron transfer mechanism involving naphthalimide (S$_1$) and the bicyclic amine.

3.2.2. Laser flash photolysis

Phototransient experiments (Nd/YAG laser; λ_{exc} = 355 nm) were performed on BNS in deaerated acetonitrile; absorption features were observed at 340, 410 and 470 nm (Fig. 4). The band at 330 nm, which mirrors ground state
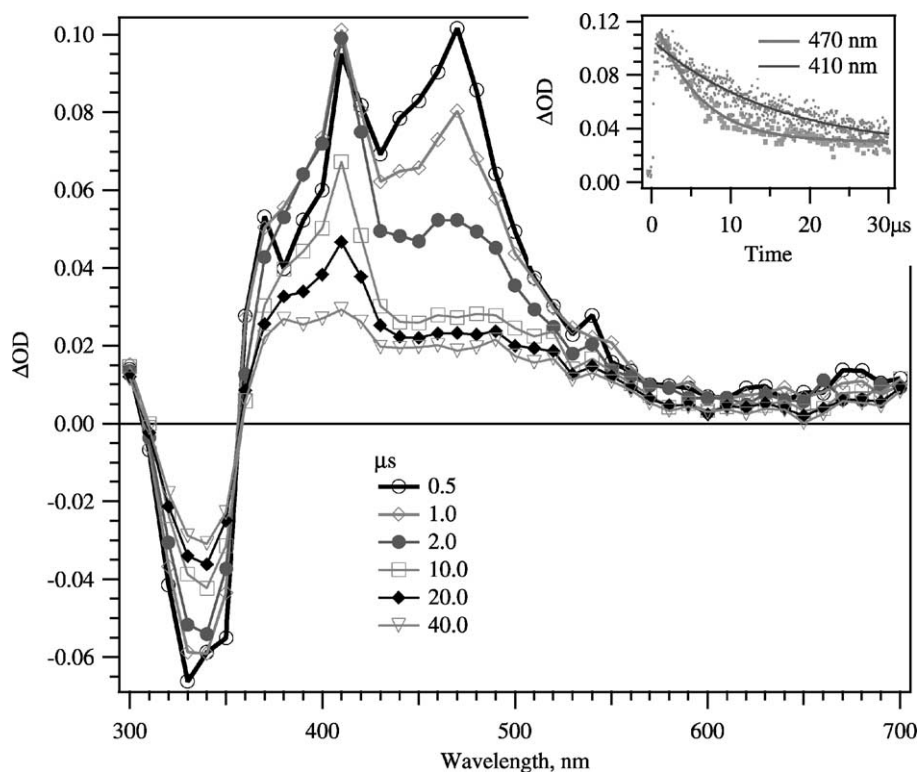
Fig. 4. Transient absorption spectra obtained on laser photolysis of BNS (36 μM, λ_{exc} = 355 nm) in deaerated acetonitrile. Inset shows decay profile of transients observed at 410 (radical anion) and 470 nm (triplet).

absorption, is due to dye bleaching and exhibits a pattern of recovery time that follows a single exponential (τ = 8.5 μs). The transient at 410 nm displays a longer decay time (τ = 12 μs) as compared to the transient observed at 470 nm (τ = 4.2 μs). Both of these transients appear at the outset of the laser pulse (ca. 10 ns). The bands at 470 and 410 nm are assigned to the naphthalimide triplet and radical anion transients, respectively, based on a comparison with reported spectral data for the species associated with simple naphthalimide structures [14,15,29].

Following the discussion above, the radical anion (410 nm transient) may arise from the following processes: (1) electron transfer from a dialkylamine (spermine) moiety to the naphthalimide monomer or (2) similar reduction by an amine moiety of naphthalimide dimer or (3) electron transfer between naphthalimide excited singlet (or triplet) state and its ground state for the associated structure (BNS). To establish which of the above processes generates these transients, flash photolysis of MNP (Scheme 1), which has a secondary amine covalently attached to a single 1,8-naphthalimide, was conducted (deaerated acetonitrile). A very weak radical anion transient (λ_{max} = 410 nm) was observed in this case along with the naphthalimide triplet. When deaerated acetonitrile solutions of BNS and MNP having the same optical density were irradiated in parallel, the relative amount of the radical anion generated in the case of BNS was about four times that of MNP (Fig. 5). The yield of the triplet generated in both cases was similar. These findings suggest that
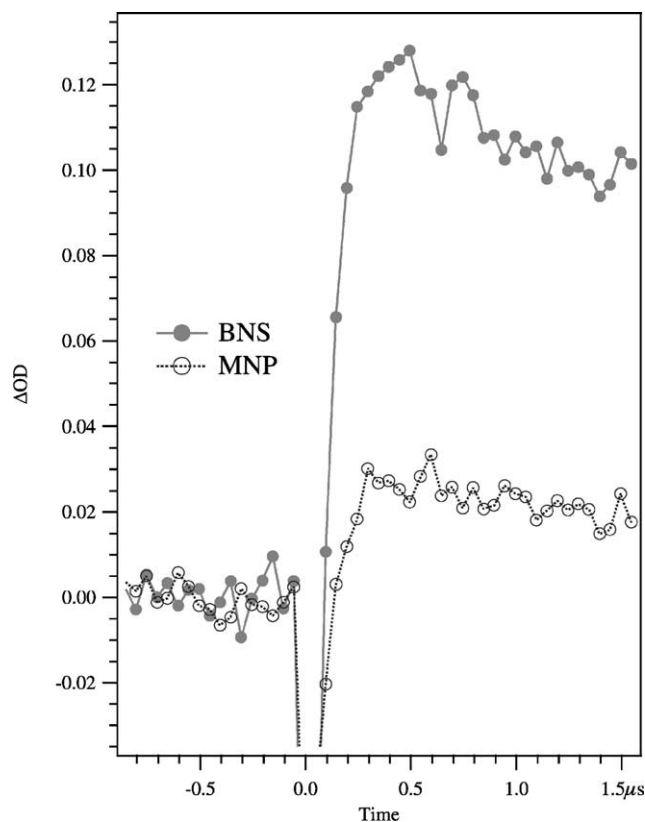

Fig. 5. Relative yield of phototransient observed at 410 nm on flash photolysis of BNS (36 μM) and MNP (100 μM) in deaerated acetonitrile (optically matched solutions; OD = 355 nm, λ_{exc} = 355 nm).
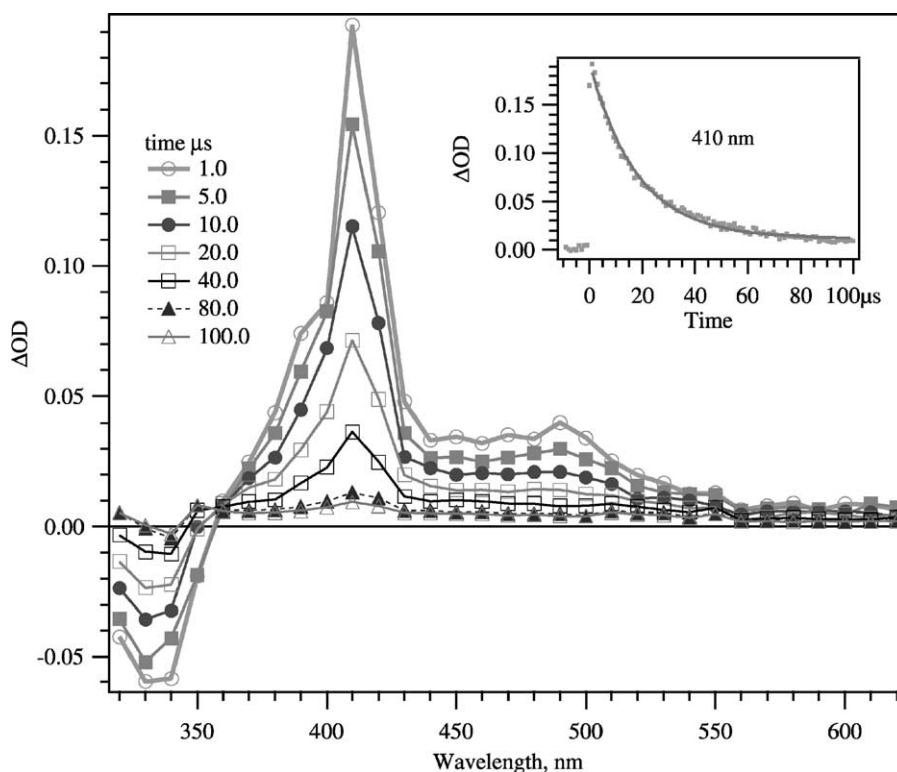
Fig. 6. Flash photolysis of BNS (36 μM, $\lambda_{exc} = 355$ nm) in deaerated acetonitrile in the presence of DABCO (9.4 mM), an electron donor. Inset shows decay of BNS radical anion at 410 nm.

the proximity of two naphthalimide rings in BNS plays a role in the generation of the radical anion transient, presumably by introducing a second electron transfer mechanism. Process 2 above should generate a dimer naphthalimide radical anion, which may not be readily distinguished from monomer radical anion (the transient absorption of naphthalimide dimer radical anion is not reported). If process 3 is operating, it should give rise to naphthalimide radical cation along with radical anion. Unfortunately, the radical cation of 1,8-naphthalimide is known to have very weak absorption that is likely not to be detectable in our experiments [15].

Flash photolysis of BNS with DABCO (9.4 mM), a good electron donor, gave exclusively naphthalimide radical anion at 410 nm ($\tau = 18$ μs), along with dye bleaching at 340 nm ($\tau = 19$ μs) (Fig. 6). No DABCO radical cation has been detected as it is reported to absorb very weakly in the region >400 nm [30]. These results further corroborate the assignment of the 410 nm transient to the naphthalimide radical anion, which arises through quenching of either BNS singlet or triplet excited states. Flash photolysis experiments of NAP (98.7 μM) in deaerated acetonitrile gave exclusively the naphthalimide triplet that is observed at 470 nm.

In a recent article, Baptista and co-workers [31] showed that a silica-gel conjugate of N,N′-bis(2-phosphonoethyl)-1,4,5,8-naphthalene diimide generates a radical anion in a process proposed to be influenced by enforced proximity of two diimide chromophores. A mechanism in which the triplet state of the dye undergoes electron transfer with the

ground state was proposed. Such a process for BNS is probably energetically unfavorable as the naphthalimide triplet state ($E_T = 2.29$ eV) lies below the value that one would estimate for the radical ion pair ($E_{RP} > 2.5$ eV, if $E_{ox} - E_{red} > 2.5$ V vs. SCE). However, such a process involving the naphthalimide excited singlet ($E_{00} = 3.51$ eV) and its ground state is feasible. According to Eq. (3), ΔG_{et} would represent a reasonable value for driving force for intra-NP pair electron transfer (i.e., $\Delta G_{et} = -0.2$ eV) if $e^2/\varepsilon r = -0.1$ eV and the "pi stacking" interaction energy, $k = -0.1$ eV. Useful as a reference is the value of the free energy of ground state dimerization, which has been experimentally determined for a pyrene chromophore that is attached to a self-assembling polypeptide (−0.13 eV) [32].

The behavior of the analog, MNP, serves to show that the NP radical anion is formed, along with diminished fluorescence, for a system composed of NP and an attached amine group in its free base form. These results are consistent with a mechanism of intramolecular electron transfer (quenching of excited NP by a proximal amine) that arises from either singlet or triplet excited states. The contrast in behavior for acidified vs. non-acidified (acetonitrile) media is illustrated in Fig. 7A which shows the prompt formation of the NP triplet (470 nm) and its decay in the microsecond time domain for MNP in its free base form. The triplet decay is considerably prolonged for MNP in acidified solution. The available redox and excitation energy data place the radical pair (RP) state that results from electron transfer somewhat
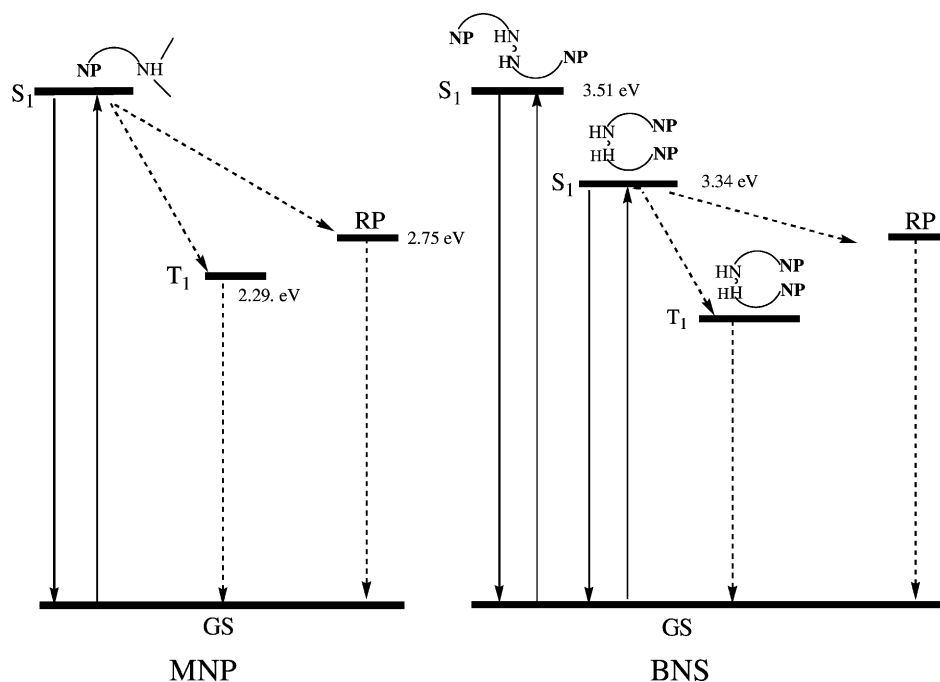
Scheme 2. Energy diagrams for BNS and MNP in acetonitrile.

above the energy of the local NP triplet (Scheme 2). Under these circumstances, the quenching of triplets should not occur or should be relatively slow; the present result may be considered analogous to the slow intermolecular quenching observed for *N*-phenyl-1,8-naphthalimide triplet and *N*,*N*-diethylamine ($k = 1.8 \pm 10^7 \, M^{-1} \, s^{-1}$) [33]. Similar decay times for both 410 and 470 nm transients of 4–6 μs are observed on flash photolysis of MNP, signaling the kinetic coupling of both singlet and triplet RP states and the MNP triplet, a situation similar to mechanisms of "triplet recombination" [34]. The general mechanism of intramolecular quenching of NP excited states by amine groups is shown in Scheme 3.

The most important observations regarding BNS photochemistry involve the conditions under which the 410 nm radical anion transie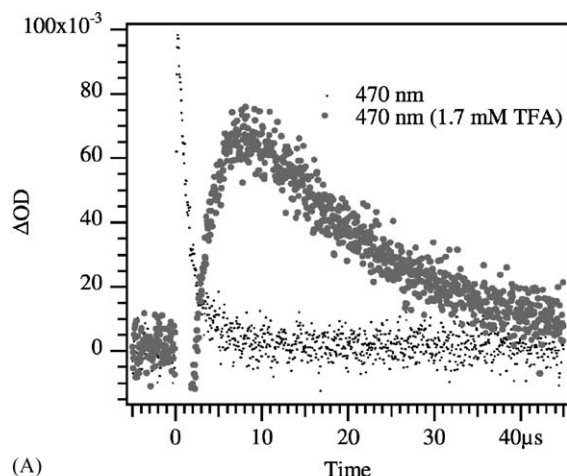nt can be observed and its enhanced yield over that observed for MNP (Fig. 5). Notably, the transient is observed on photolysis of acidified solutions with a yield that is approaching that found for unacidified media, as demonstrated by the formation and decay profiles shown in Fig. 7B. Unlike MNP, the decay profiles for RP and local triplet NP states are not similar. For BNS the 470 nm transient decays with a time constant of about 6 μs for both acidified and non-acidified acetonitrile solutions. The RP signal at 410 nm, on the other hand, exhibits a decay time of about 15 μs (Fig. 7B). The contrasting behavior for BNS can be understood in terms of a dominant pathway for radical ion formation via intra-NP-pair electron transfer in the singlet manifold (illustrated for the protonated form in Scheme 4) (there should be a lesser contribution from the amine quenching mechanism for unacidified media, Scheme 3). For this case, the relative location in energy for the local triplet and
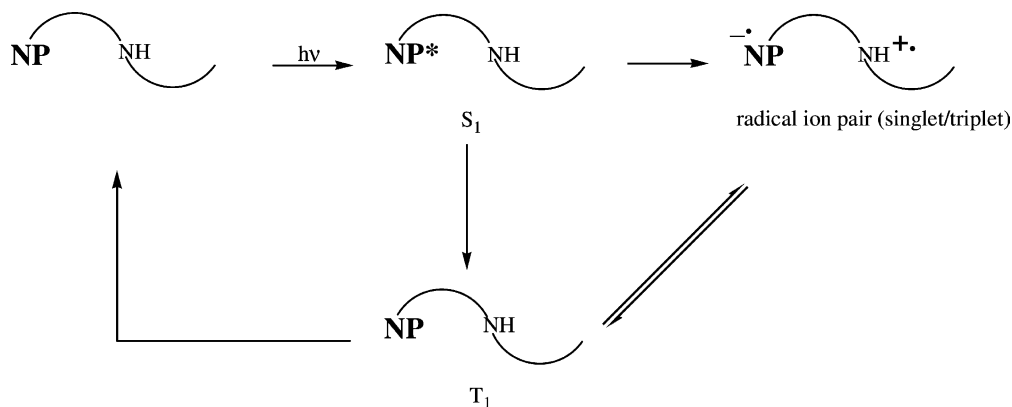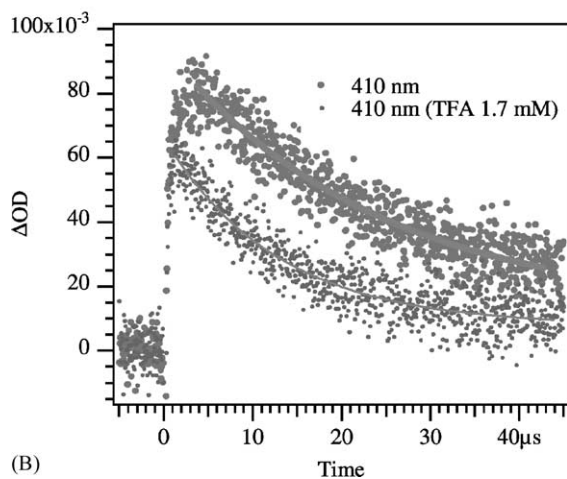

Scheme 3. Mechanism of photochemical electron transfer for MNP or BNS; either as the free base (intra-molecular amine quenching); NP: naphthalimide.
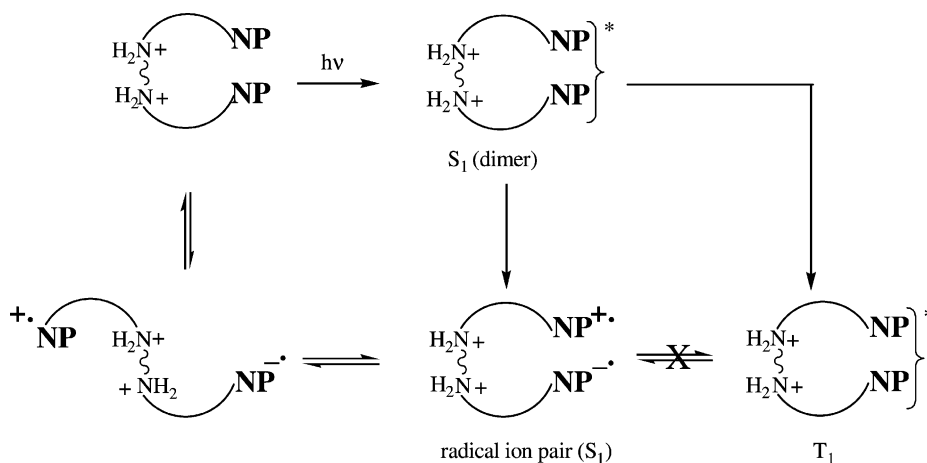
Scheme 4. Mechanism of photochemical electron transfer for BNS in protonated form (intra-NP pair quenching).

RP states is not known but the two species do not appear to be kinetically coupled. The important feature that remains is the relatively long decay time associated with the 410 radical anion transient. The time scale of the slower events is most easily associated with a radical ion pair dissociation mechanism in which the RP partners are allowed to explore geometries in which the charged species reach some average distance of separation for which back electron transfer is slowed to the tens of microseconds time scale (Scheme 4).

4. Conclusion

The photochemistry of the conjugate of N,N'-bis-1,8-naphthalimide and spermine, and two N-propyl-1,8-naphthalimide derivatives was investigated using absorption, steady-state and time-resolved emission, and transient absorption spectroscopy. In the case of the N,N'-bis-naphthalimide spermine conjugate, ground state aggregation between two pendent naphthalimide groups was detected for selected media, especially water. Naphthalimide radical anion and triplet state species were identified from the transient absorption data for BNS. The intramolecular dimer is shown to play an important role in terms of an increased yield of long-lived radical ion species on laser flash photolysis of the spermine derivative.

Acknowledgements

Fig. 7. (A) Decay curves for the 470 nm transient (NP triplet) observed on flash photolysis of MNP (100 μM, $\lambda_{exc} = 355$ nm) in deaerated acetonitrile with and without added acid (TFA). (B) The 410 nm transient (NP radical anion) for BNS (36 μM) in deaerated acetonitrile with and without added acid (TFA).

References

[1] D.S. Bendall (Ed.), Protein Electron Transfer, BIOS Scientific Publishers Limited, Oxford, 1996.

[2] S.D. Varfolomeev, I.N. Kurochkin, A.I. Yaropolov, Biosens. Bioelectron. 11 (1996) 863.

[3] P. Belser, S Bernhard, C Blum, A. Beyeler, L. De Cola, V. Balzani, Coord. Chem. Rev. 190–192 (1999) 155.

[4] A.Y. Kornilova, J.F. Wishart, W. Xiao, R.C. Lasey, A. Fedorova, Y. Shin, M.Y. Ogawa, J. Am. Chem. Soc. 122 (2000) 7999.

[5] M.W. Mutz, G.L. McLendon, J.F. Wishart, E.R. Gaillard, A.F. Corin, Proc. Natl. Acad. Sci. USA 93 (1996) 9521.

[6] C.A. Slate, D.R. Striplin, J.A. Moss, P. Chen, B.W. Erickson, T.J. Meyer, J. Am. Chem. Soc. 120 (1998) 4885.

[7] G. Jones II, V. Vullev, Org. Lett. 4 (2002) 4001.

[8] G. Jones II, X. Zhou, L.N. Lu, Tetrahedron Lett. 43 (2002) 6079.

[9] I.S. Blagbrough, S. Carrington, A.J. Geall, Pharm. Sci. 3 (1997) 223.

[10] S.A. David, R. Silverstein, C.R. Amura, T. Kielian, D.C. Morrison, Antimicrob. Agents Chemother. 43 (1999) 912.

[11] M.F. Brana, J.M. Castellano, M. Moran, M.J. Perez de Vega, D. Perron, D. Conlon, P.F. Bousquet, C.A. Romerdahl, S.P. Robinson, Anti-Cancer Drug Des. 11 (1996) 297.

[12] M.F. Brana, A. Ramos, Curr. Med. Chem. 1 (2001) 237.

[13] P.K.T. Lin, V.A. Pavlov, Bioorg. Med. Chem. Lett. 10 (2000) 1609.

[14] I. Saito, M. Takayama, H. Sugiyama, K. Nakatani, A. Tsuchida, M. Yamamoto, J. Am. Chem. Soc. 117 (1995) 6406.

[15] B.M. Aveline, S. Matsugo, R.W. Redmond, J. Am. Chem. Soc. 119 (1997) 11785.

[16] T.P. Le, J.E. Rogers, L.A. Kelly, J. Phys. Chem. 104 (2000) 6778.

[17] T. Sasaki, M. Tabet, V. Labroo, P. Sheppard, J. Am. Chem. Soc. 115 (1993) 3866.

[18] T. Cao, S.E. Webber, Macromolecule 24 (1991) 79.

[19] G. Jones II, V.I. Vullev, Photochem. Photobiol. Sci. 1 (2002) 295.

[20] A.J. Bard, L.R. Faulkner, Electrochemical Methods: Fundamentals and Applications, Wiley, NY, 1980.

[21] Y. Takeda, K. Samejima, K. Nagano, M. Watanabe, H. Sugeta, Y. Kyogoku, Eur. J. Biochem. 130 (1983) 383.

[22] T.C. Barros, G.R. Molinari, P. Berci Filho, V.G. Toscano, M.J. Politi, J. Photochem. Photobiol. A 76 (1993) 55.

[23] D. Rehm, A. Weller, Isr. J. Chem. (1970) 259.

[24] B. Uno, N. Okumura, Recent research development, Pure Appl. Chem. 2 (1998) 83.

[25] V. Vullev, G. Jones II, Tetrahedron Lett. 43 (2002) 8611.

[26] C.K. Mann, K.K. Barnes, Electrochemical Reactions in Non-aqueous Systems, Marcel-Dekker, New York, 1970.

[27] L.C.T. Shoute, J.P. Mittal, J. Phys. Chem. 97 (1993) 8630.

[28] A. Samanta, B. Ramachandram, G. Saroja, J. Photochem. Photobiol. A 101 (1996) 29.

[29] J.E. Rogers, S.J. Weiss, L.A. Kelly, J. Am. Chem. Soc. 122 (2000) 427.

[30] T. Shida, Y. Nosaka, T. Kato, J. Phys. Chem. 82 (1978) 695.

[31] M.A. Rodrigues, D.B. Tada, M.J. Politi, S. Brochsztain, M.S. Baptista, J. Non-Cryst. Solids 304 (2002) 116.

[32] G. Jones II, V.I. Vullev, J. Phys. Chem. A 105 (2001) 6402.

[33] A. Demeter, L. Biczok, T. Berces, V. Wintgens, P. Valat, J. Kossanyi, J. Phys. Chem. 97 (1993) 3217.

[34] H. Van Willigen, G. Jones II, M.S. Farahat, J. Phys. Chem. 100 (1996) 3312.